Epithermal Gold and Base Metal Mineralization at Gandy Deposit, North of Central Iran and the Role of Rhyolitic Intrusions

M. Fard, E. Rastad,[*] and M. Ghaderi

Department of Geology, Tarbiat Modares University, Tehran 14115-175, Islamic Republic of Iran

Abstract

The Gandy gold-base metal deposit is located in Tertiary Torud-Chahshirin volcano-plutonic range, north of Central Iran. Various styles of gold mineralization occur throughout the range. Mineralization at Gandy occurs in close spatial relation with rhyolitic domes in a caldera setting in a series of narrow brecciated veins. Two mineralogically and spatially different argillic alterations have affected the volcano-sedimentary host unit. The first is a pervasive advanced argillic alteration (kaolinite + quartz) and the other is a vein-controlled quartz with illite assemblage. Ore minerals comprise gold, silver, base metal sulfides and sulfosalt minerals are accompanied by carbonates, quartz and barite. Fluid inclusions in coarse-grained sphalerite have homogenization temperatures ranging from 139 to 345 °C and salinities from 7.9 to 16 wt% NaCl equiv. Data suggest that the main ore deposition mechanism is the mixing of a <200 °C and moderately low-salinity fluid resulting from condensation of magmatic volatiles in ground water with a >300 °C magmatic fluid. Mineralization at Gandy is the product of ascending gas and saline fluid exsolved from crystallizing magma, possibly due to transition from plastic into brittle regime resulting from emplacement of the rhyolitic intrusion, consequent condensation in ground water and mixing. Characteristics of the Gandy deposit are similar to those of gold and base metal-rich epithermal deposits of intermediate-sulfidation state.

Keywords: Gold and base metal epithermal mineralization; Fluid mixing; Rhyolitic intrusions; Gandy; Iran

Introduction

Iran has long been recognized as a giant metallogenic province of porphyry copper deposits. Recent discoveries of large Carlin-type, orogenic and epithermal gold deposits [1-8] especially in west and northwest of Iran, reveals an untouched gold metallogenic province as well. The Gandy gold deposit was discovered through a regional geochemical survey conducted by the Geological Survey of Iran [9]. The Gandy deposit is located at 350 km east of Tehran in the southern part of

the Torud-Chahshirin range (Fig. 1). Various styles of mineralization including quartz-base metal veins are common throughout this Tertiary volcano-plutonic range [10]. Intrusion-related gold-copper veins and associated gold placers have been mined since ancient times at Baghou-Darestan in northern part of the range [11-15] (Fig. 1).

Gandy has been mined for base metals; however, there is no reliable information on mined ore. New studies revealed high grades of gold and silver in previously mined veins, up to 285 and 680 ppm, respectively [16,17]. Mineralization occurs in a 1.5×1.2 km area and on the basis of drill holes extends to 129 meters depth. Unpublished data of the Geological Survey of Iran indicates a reserve of 5 tonnes with 6 ppm gold on average.

Method of Study

To study gold and base metal mineralization at Gandy, the deposit was mapped at 1:5000 scale. Fifty thin and polished sections were examined. In addition to nearly 2000 samples assayed by the Geological Survey of Iran, 40 chip samples were assayed for gold, silver, base metals, arsenic and antimony. X-ray diffraction, X-ray fluorescence, electron microprobe and neutron activation analyses were used to investigate chemical composition of the rocks and minerals. Fluid inclusions from eight doubly polished plates were determined and microthermometric data were collected from 6 samples.

Geological Setting

The Torud-Chahshirin range at the northern border of the Central Iran forms an uplifted block bounded by Torud Fault in the south and Anjilo Fault in the north (Fig. 1). The calc-alkaline Torud-Chahshirin volcano-plutonic complex [18], which extends over 100 km along a NE-SW belt, was emplaced during widespread Paleogene magmatic activity. The most extensive rock unit in the belt is an Eocene-Oligocene volcano-plutonic assemblage, including middle Eocene tuff, shale, marl and sandstone, middle-upper Eocene andesite and dacite and Oligocene intrusive rocks [18-20]. A within-plate geodynamic model has been suggested by Zolfaghari [19] and, Fodazi and Emami [21] for the formation of the belt. However, Jafarian [22] and Rashidnejad-Omran [13] suggested a subduction-related origin.

The lithologic units in the Gandy area include middle Eocene volcanic, volcano-clastic and terrigenous sedimentary rocks. The oldest rock units include a series of sedimentary and volcano-sedimentary rocks including conglomerate, sandstone, siltstone, marl,

evaporites, submarine rhyolitic tuff and sandy tuff, accumulated in a shallow saline lacustrine environment [23]. At the mine area, the volcano-sedimentary rocks can be grouped into two units: a lower unit composed of submarine rhyolitic tuff and sandy tuff; and an upper unit composed of zeolite-bearing marl, sandstone and rhyolitic submarine tuff. Emplacement and consequent eruption of Chekelbas andesite, north of the Gandy deposit, has resulted in the formation of a caldera (Fig. 2). Drilling has revealed that the Chekelbas andesite underlies sedimentary and volcano-sedimentary rocks. The Chekelbas andesite has a fine-grained to porphyritic texture, and is composed of plagioclase and biotite crystals in a fine-grained matrix.

The last magmatic manifestation in the Gandy area is the emplacement of rhyolitic intrusions (SiO_2>70%) in the caldera-related normal faults, possibly because of caldera resurgent volcanism. The rhyolitic intrusions are chemically similar to submarine tuffs [24] and have a fine-grained to porphyritic texture composed of quartz, alkali feldspar ± biotite in a glassy matrix. The rhyolitic intrusions, as well as most of the igneous rocks in the Torud-Chahshirin range, are calc-alkaline in composition. These rocks have strong depletions in P, Ti and Nb [24] when normalized to the composition of primitive mantle [25]. Felsic rock discrimination diagrams such as Nb *vs.* Y and Rb *vs.* Y+Nb [26] imply an island arc setting for the rhyolites (Fig. 3).
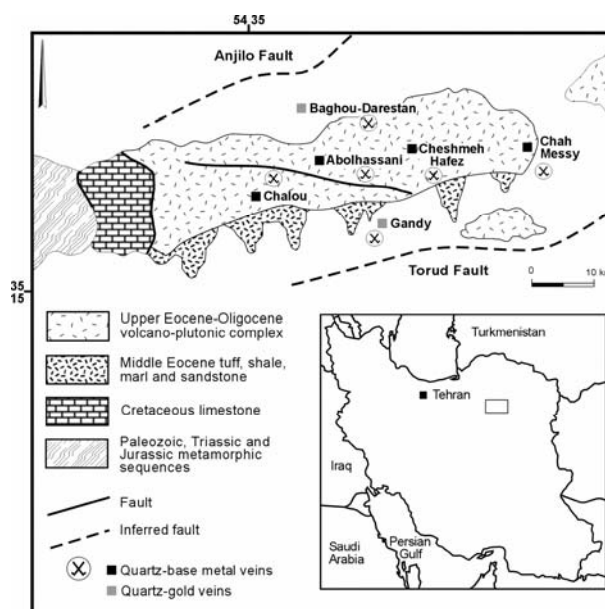

Figure 1. Simplified geological map of the Torud-Chahshirin range showing the location of quartz-base metal veins; Gandy Au (Ag+Pb+Zn+Cu), Chalou Cu (Au), Baghou-Darestan Au (Cu), Abolhassani Pb+Zn+Cu (Au), Cheshmeh Hafez Pb+Zn+Cu (Au) and Chah Messy Cu.
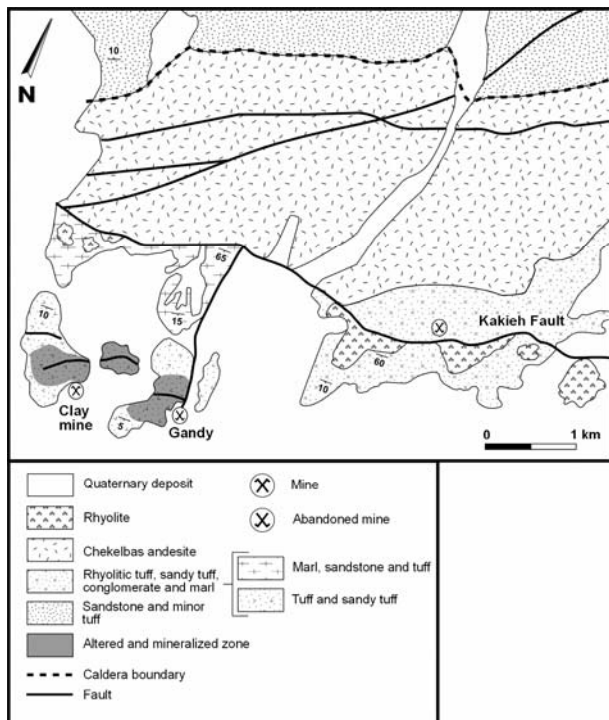
Figure 2. Geological map of the Gandy deposit showing the mineralized area located south of Kakieh normal fault.

Figure 3. Discrimination diagrams [26] for rhyolites (white diamond) and other felsic plutonic rocks (black diamond) from the Torud-Chahshirin range indicating volcanic arc setting for the igneous rocks; data from [20] and [24].

Faults, fractures, and fold axes in the region mainly trend NE-SW, parallel to the Torud and Anjilo faults. In the Gandy area, faults have a normal movement and are parallel to the trend of the calderas. Kakieh normal fault, which constitutes the southern boundary of the calderas, controls the location and emplacement of the rhyolitic intrusives (Fig. 2). Mineralization also occurs in a series of small normal faults which are parallel to the Kakieh fault in the form of veins (Fig. 2).

Alteration, Mineralization and Zoning

Two mineralogically and spatially different argillic alterations have affected the volcano-sedimentary units. The first is a pervasive advanced argillic alteration which is mined as a kaolin deposit. Mineralogy of this extensive alteration includes kaolinite and quartz. Minerals present in variable amounts including illite, clinochlore, carbonates (calcite and dolomite) and pyrophyllite. The other style is vein-controlled quartz, illite and + pyrite assemblage which occurs around the mineralized veins as one to three meter haloes (Fig. 4). Advanced argillic zone (kaolinite and quartz) where it has not been cut by the mineralized veins and veinlets is barren. Supergene jarosite, kaolinite and iron hydroxide have been developed along narrow (4-20 cm) zones around the veins. Rhyolitic intrusions also exhibit argillic alteration and silicification [27], but are poorly mineralized and the gold content of altered intrusions does not exceed 0.4 ppm (Fig. 5B). It seems that the mineralization at Gandy postdates or is synchronous with the emplacement of the rhyolitic intrusions.
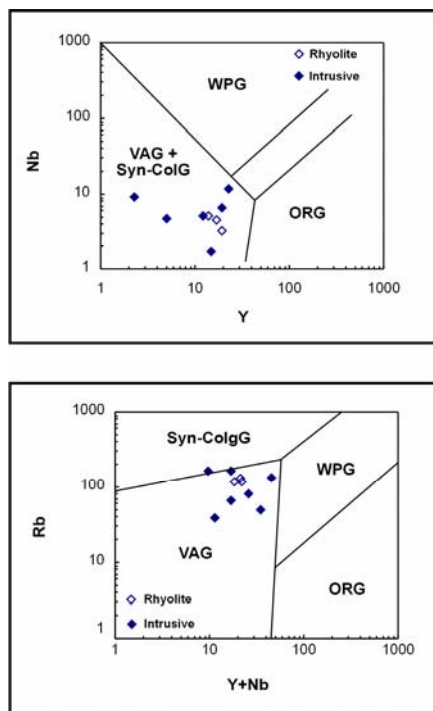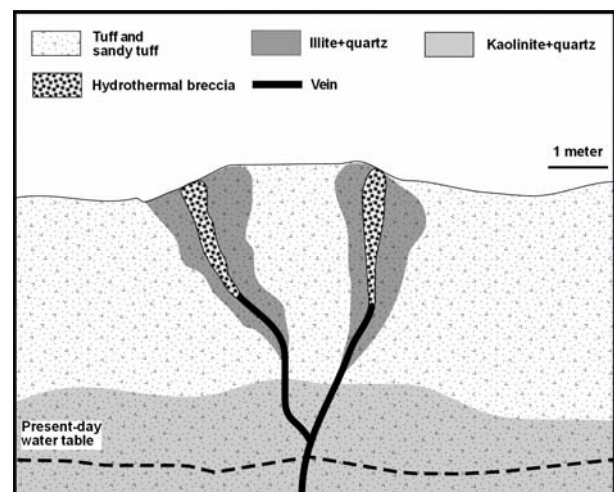

Figure 4. Illustration of two styles of alteration at the Gandy deposit; pervasive advanced argillic alteration (kaolinite + quartz) and vein-controlled illite + quartz assemblage.
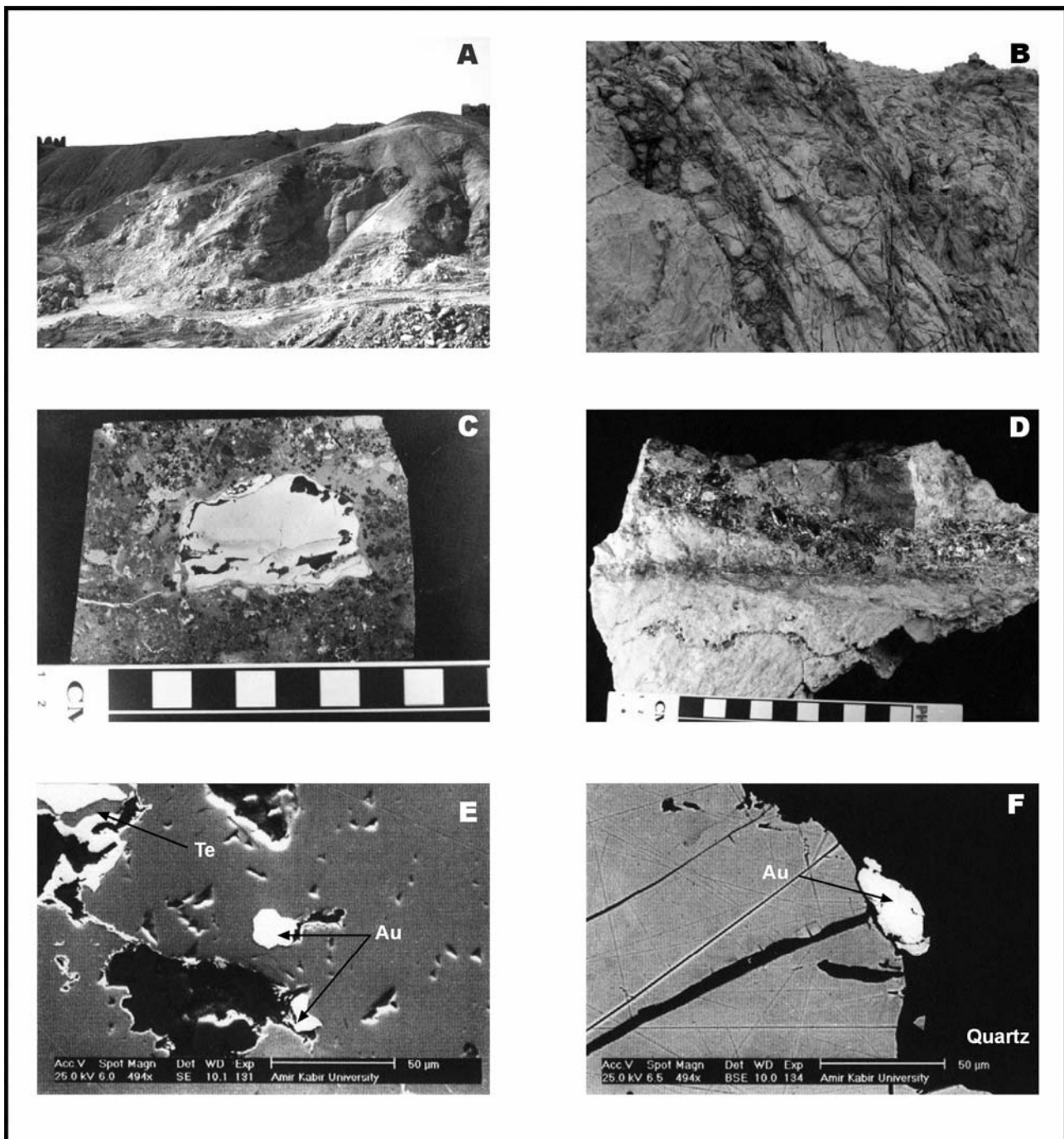
Figure 5. Alteration and mineralization at the Gandy, A. Advanced argillic alteration zone which is under mining for kaolinite. The upper red part is product of supergene oxidation of sulphides. B. Mineralization in the form of brecciated vein in one of the rhyolitic intrusions. The mineralization postdates or is synchronous with emplacement of rhyolitic intrusives. C. Hand specimen of the mineralized hydrothermal breccia which contains fragments affected by advanced argillic alteration. Sphalerite is the dominant sulfide. Brown matrix is composed of fine-grained quartz and carbonates. D. Advanced argillic alteration which is cut by mineralized vein which contains massive galena. E. Scatter electron image of gold (Au) in sphalerite. Tetrahedrite (Te) is also present in galena in the upper left corner. F. Backscatter electron image of gold (Au) inclusion in quartz next to galena.

Mineralization is characterized by sheeted-brecciated veins commonly occurring along faults. Some veins exhibit brecciated textures containing fragments of wall-rock cemented by quartz, carbonates and sulfides. Breccia fragments are not mineralized and predate precious and base metal mineralization. Silicified fragments of argillically altered rocks are present in the breccias. One hundred and ten veins have been mapped, with a total length of 5836 m, in the mine area by the Geological Survey of Iran. Vein outcrops in many locations are covered by alluvium and trenching shows long veins, in one case 225 m. The larger veins trend N30-60E and N60W and their dips range from 60 to 90°. A series of late-stage barren barite veins commonly trending N-S in the mining area cut the mineralized veins. Thickness of the veins range from 0.01 to 3.4 m (0.8 m on average) and larger veins have been mined for base metals by underground mining in the past. The maximum and average gold contents of the veins are 285 and 6 ppm, respectively.

Hypogene minerals consist of galena, sphalerite, pyrite, chalcopyrite, tetrahedrite, tennantite, silver, gold, quartz, barite, calcite, dolomite and siderite. Galena and sphalerite are the most abundant sulfides. Supergene minerals include chalcocite, covellite, malachite, azurite, iodargyrite, cerussite, smithsonite and iron oxides and hydroxides. Mineralogy of the Gandy deposit is similar to that of base metal-rich intermediate sulfidation epithermal deposits [28].

Mineralization at Gandy extends down to the Chekelbas andesite. A sharp decrease in base metal sulfides contents with depth is clear in the examined drill holes. High-grade and sulfide-rich (galena > sphalerite > pyrite > chalcopyrite) veins transform to sulfide-poor veins at depth where pyrite is the dominant sulfide. At higher levels, base metal-rich veins grade upwards into base metal-poor veins with quartz with or without gold, silver and barite. Some post-ore and mineralogically simple veins, comprising barite with or without quartz, crosscut earlier veins.

Optical and scanning electron microscope studies show the occurrence of gold in the sulfides (galena, sphalerite, and pyrite) and quartz. Gold is also reported as inclusions in chalcopyrite [29]. Gold grains are 85–91 wt% Au alloyed with Ag. Bulk samples of veins contain up to 1 wt% As and up to 0.14 wt% Sb. Antimony is present in tetrahedrite and arsenic mainly in pyrite. Sphalerite crystals exhibit weak optical and chemical zoning with FeS and CdS abundances increasing toward crystal rims, 0.8 to 1.6 and 0.2 to 0.6 mole%, respectively [30,31].

The mineralization is interpreted to have been developed in three stages. The first stage is charac-

terized by crystallization of coarse-grained As-poor pyrite and quartz with or without gold. Pyrite and quartz of this stage form euhedral to subhedral crystals. Base metal sulfides, gold and silver precipitated during the second stage. Second stage sulfides generally have overgrown the first stage pyrite and quartz crystals or have filled spaces between them. Gold is largely hosted in second stage base metal sulfides and quartz as inclusions up to 30 microns (Fig. 5E and 5F). Carbonates and minor quartz are the main gangue minerals of the second stage. Third stage minerals consist of colloform As-rich pyrite with fine-grained quartz with or without gold, silver, barite and carbonates (Fig. 6). Analyzed samples of veins and altered host rocks showed strong positive correlation between gold and base metals (Fig. 7).
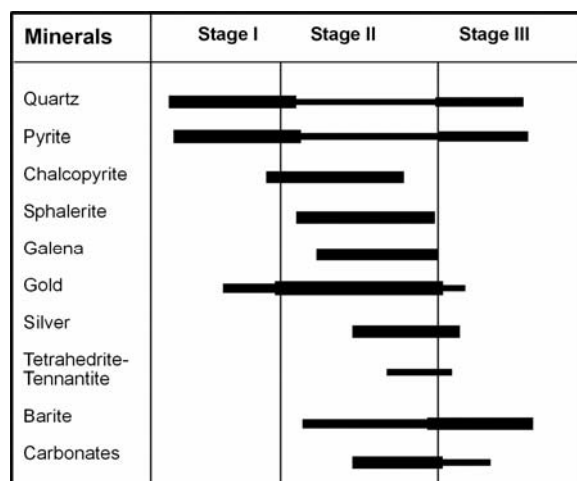

Figure 6. Diagram showing three stages of mineralization and mineral paragenesis at the Gandy deposit; gold mainly occurs in stage II base metal sulfides.
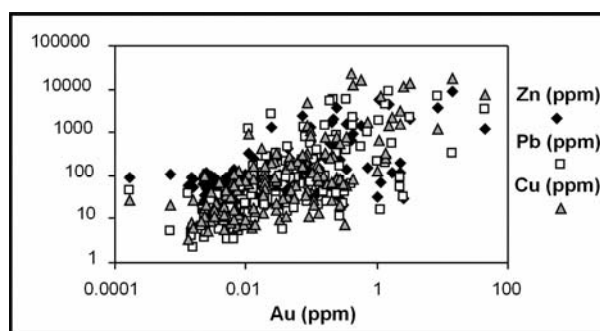

Figure 7. Variation plots for gold-base metal, in mineralized, altered and oxidized whole-rock samples and some fresh samples, which reveal high positive correlation between gold and base metals.

Fluid Inclusions

Eight doubly-polished sections were prepared for micro-thermometric measurements from the vein samples. Fluid inclusions in the quartz grains were too small (<2 microns) for measurement and data were collected from the inclusions (>4 microns) in sphalerite. Microthermometric measurements were conducted on a Linkam THMS 600 heating-cooling stage. No clathrate nucleation was observed during the cooling runs and no change was observed after ice melting.

Heating and freezing measurements were performed on primary fluid inclusions [32]. All measured fluid inclusions contained only liquid and vapour at room temperature and no daughter minerals were observed. Vapour contents ranged from less than 10% to 40% of the total volume (optical estimation). The fluid inclusions displayed a wide range of homogenization temperatures (Th) between 139 and 345 °C (Fig. 8). Final ice melting temperatures ranged from –5 to –12 °C indicative of apparent salinity [33] of 7.9–16 wt% NaCl equiv. Homogenization temperature and salinity showed a positive linear relation (Fig. 8) implying cooling and dilution of ore-forming fluids [34].

Discussion and Conclusions

Conducted studies indicate that alteration and mineralization at Gandy have been developed in two temporally different stages. The first stage has resulted in formation of the advanced argillic alteration and brecciation of the host rock, and the second stage has resulted in precious and base metal mineralization. Formation of the advanced argillic alteration and hydrothermal breccias predate precious and base metal mineralization. Here we suggest that the advanced argillic alteration and formation of hydrothermal breccias is the product of condensation of magmatic volatiles, rich in SO_2 and HCl, in the ground water, a process that is common in high-sulfidation epithermal deposits [35,36].

Condensation of magmatic volatiles in the ground water can explain formation of the alteration. Hydrothermal breccias also predate the mineralization. No mineralization was observed in the breccia clasts; however breccia clasts have been subject to the advanced argillic alteration. Formation of the hydrothermal breccias which are not widespread and are limited to some veins, especially in shallower parts of the veins, can be explained by local heating and expansion of ground water in small fractures adjacent to the main channel of fluid flow resulting in hydraulic fracturing [37].
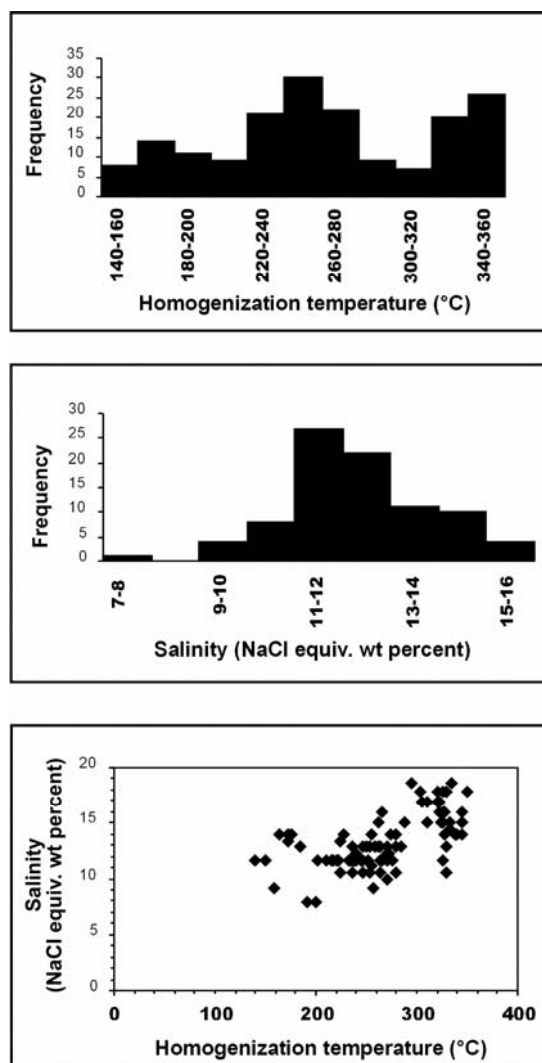

Figure 8. Histograms of homogenization temperature and salinity in sphalerite and plot of Th *vs.* Tm at the Gandy deposit revealing a mixing trend. Note that the homogenization temperature histogram is polynomial.

Precious and base metal mineralization is the product of the second stage where heated ground water, produced by condensation of magmatic volatiles in ground water, mixes with a hot magmatic fluid with higher salinity (Fig. 9). The two different stages can also be recognized in the fluid inclusions. The homogenization temperature is polynomial (Fig. 8) and most likely different fluids are responsible for mineralization. Condensation of magmatic gas in ground water at Gandy has resulted in formation of a heated (<200 °C) and corrosive ground water. Advanced argillic alteration and formation of hydrothermal breccias have been caused by this fluid. Main stage

mineralization is the product of mixing of a high-temperature magmatic fluid with the heated ground water. The Th *vs*. Tm diagram (Fig. 8) shows a dilution trend indicative of mixing between a hot and high salinity fluid and a colder and more dilute fluid.

High salinities of the low-temperature fluid inclusions (139 to 195 °C; 170 °C on average) can not be explained by condensation of magmatic volatiles in ground water since magmatic steam has low salt content [37,38]. Prior to mineralization, the Gandy area was covered by a shallow and saline lake [23], in which evaporites have been deposited along with terrigenous and volcanic layers. An acceptable explanation for high-salinity of fluid inclusions at Gandy is the possible role of lake water in mineralization. Solution of salt from evaporites into the ground water can be another explanation.

The high salinities of fluid inclusions at Gandy are also comparable with data presented by Albinson *et al.* [39] for base metal-rich epithermal deposits in Mexico and Bereznjakovskoje gold trend in Russia [40]. According to Albinson *et al.* [39] subtypes of epithermal deposits, gold-silver (<3.5 wt% NaCl equiv.), gold-rich Ag-Pb-Zn (8.4 to 14.4 wt% NaCl equiv.) and base metal-rich silver-gold (as high as 23 wt% NaCl equiv.), reveal progressively higher salinities. Fluid inclusions and mineralogical characteristics of the Gandy deposit present similarities with the base metal-rich epithermal subtype (*e.g.*, Colorado, Topia and La Guitarra in Mexico) [39]. However, high temperature of formation, lack of epithermal textures, and abundance of carbonates are characteristic of distal intrusion-related carbonate-base metal deposits.

There is no fluid inclusion evidence for boiling at Gandy such as co-genetic liquid- and vapour-rich inclusions [41]. Mineralogical evidence for boiling such as presence of adularia, lattice calcite and crustiform-colloform amorphous silica [42-44] are also absent. Shamanian *et al.* [30,31] suggested the occurrence of mineralized breccias as boiling indicator in some parts of the Gandy deposit. Fluid inclusion trapping pressure and depth could not be estimated because of the lack of boiling assemblages [45]. Fluid inclusions with homogenization temperatures from 200 to 300 °C, however, give a minimum trapping depth of 390 m below the paleo water-table [46].

We discussed that the advanced argillic alteration and formation of hydrothermal breccias are the product of condensation of magmatic volatile in the ground water. Chekelbas andesite underlies the Gandy deposit and mineralization extends into it. Hence, it can be suggested as a source of mineralizing agents (Fig. 9). The question here is the role of rhyolitic intrusions in

mineralization at Gandy which are altered and partly mineralized (Fig. 5B). Here we suggest that gold and base metal mineralization at the Gandy deposit is related to the emplacement of rhyolitic intrusion in the host sequences.

Close association of felsic rocks and gold mineralization have long been recognized. Spatial and temporal association of rhyolitic rocks and gold mineralization is documented in several mining districts including Sunnyside, Idarado and Camp Bird [47] in USA and Patagonia [48] in Argentina. In some deposits, rhyolites are the main host rock [48] and where the rhyolites are not the host rock, they have been considered as a source for gold [47].
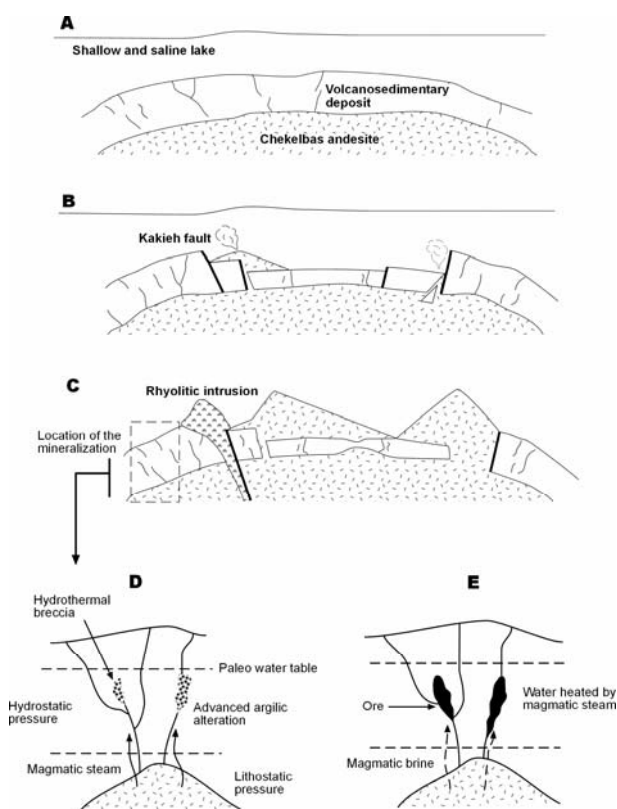

Figure 9. Geological events that have led to mineralization at Gandy, A. Emplacement of Chekelbas andesite has resulted in doming of volcanosedimentary layers in a shallow lake. B. Eruption of Chekelbas andesite has resulted in collapse of volcanosedimentary layers, formation of a caldera and developing a series of normal faults including Kakieh fault. C. Emplacement of rhyolitic intrusions along caldera related normal faults and subsequent mineralization. D and E. Emplacement of rhyolitic intrusions results in increase in local strain rate resulting in breaching of sealed zone dividing lithostatic from hydrostatic domain and allows brine and gas to be expelled quickly to the epithermal environment and cause the observed mineralization.

The host rock of the Gandy deposit is submarine rhyolitic tuff, a favorable host for epithermal gold deposits [35], which has been deposited in a shallow and saline lake prior to the emplacement of the Chekelbas andesite (Fig. 9). The Chekelbas andesite which is considered as a source of mineralizing agent has been intruded later by rhyolitic intrusions. Evidence at the Gandy deposit suggests that the role of rhyolitic intrusion is not to provide metals or fluids. It seems that the intrusion of rhyolitic intrusives increased local strain rate in a crystallizing magma chamber where Chekelbas andesite was under crystallization. The intrusion has resulted in breaching the sealed zone dividing lithostatic realm from hydrostatic domain resulting in alteration and mineralization in the overlying epithermal environment [37]

Acknowledgements

References

1. Assadi H.H., Voncken J.H.L., Kuhnel R.A., and Hale M. Petrography, mineralogy and geochemistry of the Zarshuran Carlin-like gold deposit, northwest Iran. *Miner. Deposita*, **35**: 656-671 (2000).
2. Daliran F., Walther J., and Stuben D. Sediment-hosted disseminated gold mineralization in the North Takab geothermal field, NW Iran. In: Stanley C.J. (Ed.), *Mineral Deposits: Processes to Processing*, p. 837-840 (1999).
3. Mehrabi B., Yardley B.W.D., and Cann J.R. Sediment-hosted disseminated gold mineralization at Zarshuran, NW Iran. *Miner. Deposita*, **34**: 673-696 (1999).
4. Hassani-Pak A. Systematic geochemistry report on 1:100,000 Alout geological map. Geological Survey of Iran: Internal Report, in Persian (1998).
5. Hassani-Pak A. Systematic geochemistry report on 1:100,000 Tijtij geological map. Kordestan Province Department of Mines and Metals: Internal report, in Persian (1999).
6. Mohajjel M. and Shamsa M.J. Rock fabric in Kervian gold deposit (40 km southwest of Saghez). 20th Symposium on Geosciences, Geological Survey of Iran, Tehran, CD-ROM, in Persian (2001).
7. Heydari M., Rastad E., Mohajjel M., and Nabian A. Gold mineralization in Kervian altered shear zone. 21th Symposium on Geosciences, Geological Survey of Iran, Tehran, CD-ROM, in Persian (2003).
8. Rastad E., Niroumand S.A., Emami M.H., Rashidnejad-and Omran N. Genesis of Sb-As-Au deposit in Dashkasan volcano-plutonic complex (east Qorveh, Kordestan province). *Iranian Geosciences Journal*, **37-38**: 2-23, in Persian (2002).
9. Geological Survey of Iran. Explanatory text of geochemical map of Moaleman (6960). Report no. 9: 33 p. (1995).
10. Abedian N. and Dorri M.B. Copper exploration in Semnan province. Semnan Department of Industries and Mine, 194 p., in Persian (1996).
11. Fard M., Rastad E., Rashidnejad-Omran N., and Ghaderi M. Mineralization and potential of gold in Torud-Chahshirin volcano-plutonic complex (south Damghan). Proceedings of the 5th Symposium of Geological Society of Iran, pp. 214-217, in Persian (2001).
12. Moore F. and Shakeri A. Geology, mineralogy and fluid inclusion study of Baghou vein type gold deposit. Proceedings of the 4th Symposium of Geological Society of Iran 1, pp. 325-328, in Persian (2000).
13. Rashidnejad-Omran N. Petrology and magmatic evolution of igneous rocks in the Baghou and its relation to gold mineralization. Unpublished M.Sc. Thesis, Tarbiat Moalem University, 255 p., in Persian (1992).
14. Rastad E., Tajeddin H., Rashidnejad-Omran N., and Babakhani A. Genesis and gold (copper) potential in Darestan-Baghou mining area. *Iranian Geosciences Journal*, **35-36**: 60-79, in Persian (2000).
15. Tajeddin H. Geology, mineralogy, geochemistry and genesis of Darestan gold occurrences (south Damghan). Unpublished M.Sc. Thesis, Tarbiat Modares University, 236 p., in Persian (1999).
16. Borna B. and Eshghabadi M. Exploration and assessment report on lead and zinc deposits of Semnan province. Semnan Department of Industries and Mines, 226 p., in Persian (1998).
17. Kosari S. Detailed geochemical exploration in Gandy mining area, Geological Survey of Iran, Internal report, in Persian (2001).
18. Houshmandzadeh A., Alavi M., and Haghipour A. Geological evolution of Torud (from Precambrian to recent). Geological Survey of Iran, 138 p., in Persian (1978).
19. Zolfaghari S. Petrology of Eocene volcanic rocks of Moaleman region, Damghan, Unpublished M.Sc. Thesis, Islamic Azad University, 157 p., in Persian (1998).
20. Kohansal R. Petrology of late Eocene-Oligocene plutonic rocks of Moaleman region, Damghan. Unpublished M.Sc. Thesis, Islamic Azad University, 224 p., in Persian (1998).
21. Fodazi M. and Emami M.H. Petrology of Mabad Tertiary magmatic rocks (northwest Torud, Central Iran). 18th Symposium on Geosciences, Geological Survey of Iran, Tehran, pp. 224-229, in Persian (2000).
22. Jafarian A. Petrology of Kuh Zar-Torud volcano-plutonic arc and related mineralization. Unpublished M.Sc. Thesis, University of Tehran, in Persian (1988).
23. Eshraghi S. 1:20,000 Geological map and report of Moaleman area. Geological Survey of Iran, in Persian (1998).
24. Fard M. and Rastad E. Characteristics of rhyolites in the

southern part of Torud-Chahshirin volcano-plutonic complex and their relation to epithermal gold-base metal mineralization at Gandy mining area. 20th Symposium on Geosciences, Geological Survey of Iran, Tehran, CD-ROM, in Persian (2002).

25. Sun S.S., McDonough W.F. Chemical and isotopic systematics of oceanic basalts: Implications for mantle composition and processes. *Geological Society of London Special Publication*, **42**: 313-345 (1989).

26. Pearce J.A., Harris N.B.W., and Tindle A.G. Trace element discrimination diagrams for the tectonic interpretation of granitic rock. *J. Petrol.*, **25**: 956-938 (1984).

27. Fard M., Rastad E., Mehrparto M., and Ghaderi M. Geology, mineralogy and alteration at Gandy epithermal gold-base metal deposit (southeast Damghan) Proceedings of the 5th Symposium of Geological Society of Iran, pp. 248-251, in Persian (2001).

28. White N.C. and Hedenquist J.W. Epithermal gold deposits: Styles, characteristics and exploration. *Society of Economic Geologists Newsletter*, **23**: 9-13 (1995).

29. Golyai S. Economic geology of metallic deposits in Moaleman, Damghan. Unpublished M.Sc. Thesis, Islamic Azad University, 138 p., in Persian (1999).

30. Shamanian G.H., Hassanzadeh J., Hedenquist J.W., Hattori K.H., Ghaderi M. Comparison of epithermal base and precious metal deposits in Gandy and Abolhassani districts, Semnan province, Iran. *Iranian Geosciences Journal*, **12**: 100-117, in Persian (2004a).

31. Shamanian G.H., Hedenquist J.W., Hattori K.H., and Hassanzadeh J. The Gandy and Abolhassani epithermal deposits in the Alborz magmatic arc, Semnan Province, northen Iran. *Econ. Geol.*, **99**: 691-712 (2004b).

32. Roedder E. Fluid inclusions. Mineralogical Society of America, Reviews in Mineralogy, **12**: 644 p. (1984).

33. Bodnar R.J. Revised equation and table for determining the freezing point depression of H_2O-NaCl solutions. *Geochim. Cosmochim. Acta*, **57**: 683-684 (1993).

34. Hedenquist J.W. and Henley R.W. Effect of CO_2 on freezing point depression measurements of fluid inclusions: Evidence from active systems and application to epithermal studies. *Econ. Geol.*, **80**: 1379-1406 (1985).

35. Hedenquist J.W., Arribas A.Jr., and Gonzalez-Urien E. Exploration for epithermal gold deposits. *Society of Economic Geologists Reviews*, **13**: 245-277 (2000).

36. Sillitoe R.H. Style of high-sulfidation gold, silver and copper mineralization in porphyry and epithermal environments. PacRim99, Proceedings, pp. 29-44 (1999).

37. Fournier R.O. Hydrothermal processes related to movement of fluid from plastic into brittle rock in the magmatic-epithermal environment. *Econ. Geol.*, **94**: 1193-1211 (1999).

38. Hedenquist J.W., Arribas A.Jr., and Raynolds T.J. Evolution of an intrusion-centered hydrothermal system: Far Southeast-Lepanto porphyry and epithermal Cu-Au deposits, Philippines. *Ibid.*, **93**: 373-404 (1998).

39. Albinson T., Norman D.I., Cole D., Chomiak B. Controls on formation of low-sulfidation epithermal deposits in Mexico: Constraints from fluid inclusion and stable isotope data. *Society of Economic Geologists Special Publication*, **8**: 1-32 (2001).

40. Lehmann B., Heinhorst J., Hein U., Neumann M., Weisser J.D., and Fedesejev V. The Bereznjakovskoje gold trend, southern Urals, Russia. *Miner. Deopsita*, **34**: 241-249 (1999).

41. Bodnar R.J., Reynolds T.J., and Kuehn C.A. Fluid inclusion systematics in epithermal systems. In: Berger B.R., Bethke P.M. (Eds.), *Geology and Geochemistry of Epithermal Systems: Reviews in Economic Geology*, **2**: pp. 73-79 (1985).

42. Cooke R.C. and Simmons S.F. Characteristics and genesis of epithermal gold deposits. *Society of Economic Geologists Reviews*, **13**: 221-244 (2000).

43. Simmons F.S. and Brown P.R.L. Hydrothermal minerals and precious metals in the Broadlands-Ohaaki geothermal system: implication for understanding low-sulfidation epithermal environments. *Econ. Geol.*, **95**: 971-999 (2000).

44. Simmons S.F., Mauk J.L., and Simpson M.P. The mineral products of boiling in the Golden Cross epithermal deposit. New Zealand Minerals & Mining Conference Proceeding. 29-31 October 2000 (2000).

45. Shepherd T.J., Rankin A.H., Alderton D.H.M. A practical guide to fluid inclusion studies. Blackie, London, 238 p. (1985).

46. Haas J.L. The effect of salinity on maximum thermal gradient of a hydrothermal system at hydrostatic pressure. *Econ. Geol.*, **66**: 940-946 (1971).

47. Bartos P.J. Comparison of gold-rich and gold-poor quartz-base metal veins, western San Juan Mountains, Colorado: the Mineral Point area as an example. *SEG Newsletter*, **15**: 6-11 (1993).

48. Haller M.J. The rhyolite field related gold deposits from Patagonia. In: Papunen, H. (Ed.), *Mineral Deposits: Research and Exploration – Where Do They Meet*. Balkema, Rotterdam, pp. 201-203 (1997).